

Theoretical considerations on the anhysteretic remanent magnetization of interacting particles with uniaxial anisotropy

R. Egli¹

Received 16 June 2006; revised 25 October 2006; accepted 30 October 2006; published 7 December 2006.

[1] The anhysteretic remanent magnetization (ARM) is widely used in rock magnetism and paleomagnetism because of its sensitivity to the domain state of magnetic particles and the close analogy to natural remanent magnetizations. On the other hand, the ARM shares with other weak-field magnetizations the property of being extremely sensitive to magnetostatic interactions. Therefore it is desirable to model the effects of interactions on natural assemblages of magnetic particles. Direct micromagnetic calculations of the ARM acquisition process are not practicable; therefore an analytical approach is used to calculate the ARM susceptibility of a system of interacting single-domain (SD) particles. The model is based on a statistical description of the interaction field. The equations obtained have been used to evaluate the dependence of the ARM on the packing fraction of the magnetic particles. The effect of interactions on the anisotropy of ARM (AARM) was evaluated as well. The AARM of densely packed particles is complex and depends critically on the microcoercivity. A physical interpretation of the AARM of highly interacting particles is therefore difficult.

Citation: Egli, R. (2006), Theoretical considerations on the anhysteretic remanent magnetization of interacting particles with uniaxial anisotropy, *J. Geophys. Res.*, *111*, B12S18, doi:10.1029/2006JB004577.

1. Introduction

[2] The anhysteretic remanent magnetization (ARM) has been since long time a subject of investigation in association with magnetic recording materials [e.g., *Eldridge*, 1961; *Kneller*, 1968; *Jaep*, 1969; *Walton*, 1990]. At the same time, the ARM has been used as a grain size indicator in rock magnetism [e.g., *Johnson et al.*, 1975; *King et al.*, 1982], and as a normalization factor in paleointensity studies [e.g., *Shaw*, 1974; *Rolph and Shaw*, 1985]. The anisotropy of ARM (AARM) has found application in sediments for correction of inclination shallowing of detrital remanent magnetization [e.g., *Jackson et al.*, 1991; *Kodama and Sun*, 1992; *Kodama*, 1997]. More recently, ARM magnetization curves have been used to quantify magnetofossils in freshwater and marine sediments [*Egli*, 2004].

[3] The ARM is a complicated magnetic acquisition process that is extremely sensitive to the size of the magnetic particles, and to magnetostatic interactions [*Egli and Lowrie*, 2002; *Sugiura*, 1979]. These properties are shared with other weak-field magnetizations, such as the thermoremanent and the chemical remanent magnetization [*Néel*, 1949, 1955; *Shcherbakov et al.*, 1996]. It is not surprising that modeling of weak-field magnetizations is an extremely difficult task, especially if magnetostatic interactions are included. However, precise quantitative models

are desirable to correctly reveal differences between various types of magnetizations and their grain size dependence.

[4] Models for the ARM of noninteracting single-domain (SD) particles have evolved from early Preisach models [*Wohlfarth*, 1964] to an approach based on thermal activation effects [*Walton*, 1990], which lead to a complete analytical solution [*Egli and Lowrie*, 2002]. On the other hand, *Xu and Dunlop* [1995] developed a model for the ARM acquisition in multidomain grains. Other properties such as the additivity and reciprocity of partial ARM [*Yu et al.*, 2002a, 2002b], and the dependence of the ARM on the decay rate of the alternating field [*Yu and Dunlop*, 2003], have been investigated.

[5] Recent advances in micromagnetic calculations allow modeling the effect of magnetostatic interactions on the hysteresis properties of interacting particles [*Muxworthy et al.*, 2003], and first-order reversal curves (FORC) gained increasing interest as a tool to characterize interactions in rocks and sediments [*Roberts et al.*, 2000]. On the other hand, the theoretical investigation of the effects of magnetostatic interactions on the ARM remains limited to studies of highly ordered magnetic recording materials [e.g., *Wohlfarth*, 1964; *Papusoi and Stancu*, 1993; *Della Torre and Vajda*, 1997]. A micromagnetic modeling of interaction effects on the ARM is computationally too demanding, since it requires one to calculate the magnetization of thousands of particles along a high-resolution time scan of a typical alternating field cycle. Monte Carlo methods provide a practical approach to modeling of weak-field magnetizations of interacting particles, as shown by *Shcherbakov et al.* [1995].

¹Institute for Rock Magnetism, University of Minnesota, Minneapolis, Minnesota, USA.

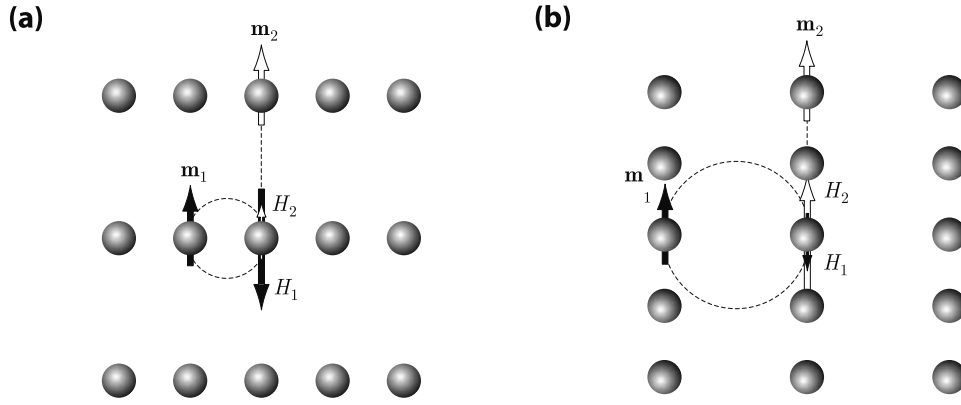


Figure 1. Schematic representation of magnetic particles with (a) a negative mean interaction field and (b) a positive mean interaction field. Field lines are dashed, H_1 and H_2 are the z components of the dipole field produced by \mathbf{m}_1 and \mathbf{m}_2 .

[6] In this paper, a fully analytical model of the ARM of a random set of interacting SD particles is presented. A so-called moving Preisach approach [Hejda and Zelinka, 1990] is used to calculate the magnetic field acting on each particle during the ARM acquisition, supported by a general statistical model for the local interaction field (IF) [Egli, 2006]. An interesting outcome of the model is the fact that the ARM susceptibility of interacting particles is a strong function of only three parameters: the noninteracting susceptibility, the saturation magnetization of the particles, and their volume density. The analytical model provides a direct means to calculate the effects of interactions on the anisotropy of ARM (AARM) in terms of geometrical parameters that describe an orientation-dependent distribution of particles in space, called “distribution anisotropy” is similar studies on the anisotropy of magnetic susceptibility [e.g., Stephenson, 1994].

2. Statistical Description of the Interaction Field

[7] Without loss of generalization, let us consider the IF produced by an assemblage of interacting particles along a given direction, assumed to be the z axis of a coordinate system. The z component H_i of the IF acting on a magnetic particle is conveniently described by

$$H_i = H_z + H_d + H_m \quad (1)$$

where H_z and H_m are the random and the mean components of the local interaction field, respectively, and H_d is the demagnetizing field. The demagnetizing field is given by $H_d = -f_d M$, where f is the demagnetizing factor [Osborn, 1945], and M is the magnetization of the sample. For a spherical sample, $f = 1/3$. The random component of the IF is different for each grain in the sample, and is therefore treated as a statistical variate characterized by a probability density function (PDF) $W(H_z)$ [Shcherbakov and Shcherbakova, 1975; Berkov, 1996]. If the typical distance between SD grains is larger than their diameter, the random component of the IF corresponds with good approximation to the sum of the dipole fields produced by all grains. Egli [2006] obtained following PDF for the IF produced by an

isotropic assemblage of random dipoles along a given direction:

$$W(H_z; p, \mu_s) = \frac{e^{\alpha\beta}}{\pi\beta\sqrt{1+H_z^2/\alpha^2}} K_1\left(\frac{\alpha}{\beta}\sqrt{1+H_z^2/\alpha^2}\right) \quad (2)$$

where p is the packing fraction (i.e., the volume occupied by the particles divided by the total volume of the sample), μ_s is the saturation magnetization of the particles, K_1 is the modified Bessel function of the second kind, and α , β are two parameters that depend on p . For small packing fractions $0 < p \leq 0.01$, (2) is conveniently approximated by the Lorentz (also called Cauchy) distribution:

$$C(H_z, p\mu_s) = \frac{1}{\pi\alpha_0 p\mu_s \left[1 + \frac{H_z^2}{(\alpha_0 p\mu_s)^2}\right]} \quad (3)$$

$$\alpha_0 = \frac{\pi}{12} \left[\frac{\ln(2 + \sqrt{3})}{2\sqrt{3}} + 1 \right] \approx 0.361$$

Both distributions in (2) and (3) are even functions that describe a statistical variate with zero mean. The mean component $H_m = f_m M$ of the local IF describes the net balance between positive and negative interactions, whereby the notation “positive” and “negative” refer to the sign of the scalar product between interaction field and magnetization. In a sample of isotropic dispersed grains, positive and negative interactions are balanced, and $f_m = 0$ follows from Gauss’s theorem. If the average distance between the particles is smaller (larger) along the direction of measurement, f_m is positive (negative). Examples of configurations leading to $f_m \neq 0$ are shown in Figure 1. These configurations introduce an anisotropy of the magnetic properties due to interactions, called “distribution anisotropy” [e.g., Muxworthy and Williams, 2004]. If the easy axes of the particles are randomly oriented, positive interactions are predominant along the direction of shortest distance between the particles ($f_m > 0$), and negative interactions are predominant along the direction of largest distance between the particles ($f_m < 0$).

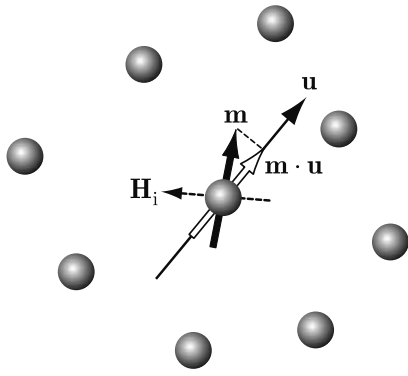


Figure 2. Schematic representation of the randomizing effect of the local IF H_i on a magnetic moment \mathbf{m} , which is deflected from the easy axis \mathbf{u} . The total magnetization is given by the sum of all components $\mathbf{m} \cdot \mathbf{u}$ of the magnetic moment along the easy axes.

[8] An anisotropic distribution of the particles is also expected to produce a direction-dependent PDF of the random component of the IF. This effect can be easily understood in the limit case of isolated, aligned “strings” of SD particles, where the calculation of the IF is reduced to a one-dimensional problem. In more realistic cases of slightly anisotropic configurations, the random component of the IF is described by (2) or (3), whereby the scalar parameters α and β are replaced by tensors. The calculation of α and β for anisotropic cases is not straightforward, and will be the subject of future research.

[9] If all contributions to the IF are taken into account, the total field acting on a magnetic grain is completely described by the PDF $W(H + H_z - fM; p, \mu_s)$, where H is an external applied field, and $f = f_d - f_m$.

3. Statistical Effects of the IF on the Remanence

[10] One of the main difficulties in modeling interacting assemblages is that it is a highly nonlinear problem which cannot be treated analytically in the general case. A drastic simplification of the problem is possible in the case of weak-field magnetizations, such as ARM, which are much weaker than the saturation magnetization of the sample. In this case, as I will show in section 4, the total magnetization of a sample can be expressed in terms of the switching states of the individual particles.

[11] Consider an interacting assemblage of uniaxial, SD particles in an initially demagnetized state. A remanent magnetization is acquired by switching the magnetic moments of a subset of all particles. If magnetostatic interaction effects are ignored, the magnetic moments are aligned with the corresponding easy axes, giving a net remanent magnetization M_0 . Under the influence of the IF, the magnetic moments are deflected from the easy axes to an extent that depends on the ratio of the IF amplitude to the microcoercivity H_K of the particles. Moreover, the IF can be strong enough to switch the moment of some particles. Macroscopically, these effects can be accounted by multiplying M_0 by a factor $\xi = \xi_m(M)\xi_r(p)$, where

$\xi_m(M)$ and $\xi_r(p)$ represent the effects of the mean and the random part of the IF, respectively. If the ARM is acquired in a small field h , the mean IF is given by $H_m = -f\chi_{ai} h < h$, where χ_{ai} is the susceptibility of ARM. As it will be shown in section 4, an upper limit for χ_{ai} is given by $\chi_{ai} = f^{-1}$, which coincides with an early result obtained by *Wohlfarth* [1964]. Since typical fields used for ARM experiments are of the order of magnitude of 0.1 mT, $H_m < h \ll H_K$ is always a valid assumption, and the mean IF can be neglected. Therefore $\xi_m \equiv 1$ will be used in the following.

[12] A rigorous calculation of ξ_r is obtained by minimizing the normalized energy ε of a uniaxial SD grain subjected to a random IF:

$$\varepsilon(\theta) = \sin^2 \theta - 2(h_x \sin \theta + h_z \cos \theta) \quad (4)$$

where θ is the angle between the magnetic moment and the easy axis, and $h_x = (H_x + H_y)^{1/2}/H_K$ and $h_z = H_z/H_K$ are the normalized components of the IF perpendicular, respectively parallel to the easy axis. Each component is a statistical variate with PDF given by equation (1). Since the deviations of the magnetic moments \mathbf{m} from the easy axes \mathbf{u} are random, the total magnetization of the sample is given by summation of the components $\mathbf{m} \cdot \mathbf{u}$ along the easy axes (Figure 2). The factor $\xi_r(p)$ is obtained from a weighted integration of $\mathbf{m} \cdot \mathbf{u}$ over all possible configurations of the IF:

$$\xi_r(H_K, p) = \int_{-\infty}^{+\infty} W(H_K h_x) \int_{-\infty}^{+\infty} W(H_K h_y) \cdot \int_{-\infty}^{+\infty} W(H_K h_z) \cos \theta_m dh_z dh_y dh_x \quad (5)$$

where θ_m minimizes (4), and $\mathbf{m} \cdot \mathbf{u} = \cos \theta_m$. The integral in (5) must be evaluated numerically, since the minimization of (4) does not have an analytical solution. The limits $\xi_r(p \rightarrow 0, H_K) = 1$ and $\xi_r(p, H_K \rightarrow 0) = 0$ of (5) characterize the cases of noninteracting particles on one hand, and interacting superparamagnetic particles on the other (Figure 3). *Muxworthy et al.* [2003] used a micromagnetic model to calculate the effect of magnetostatic interactions on the hysteresis parameters of a regular array of interacting particles. Their results for the remanence ratio M_{rs}/M_s of uniaxial SD particles show the same trend predicted by (5), whereby M_{rs}/M_s decreases with increasing packing fractions.

4. Acquisition of Anhyseretic Remanent Magnetization

[13] An ARM is acquired by applying an alternating field $\vec{H}(t) \cos \omega t + h$ with bias h and a linearly decreasing amplitude $\vec{H}(t) = \vec{H}_0(1 - \eta t)$, where η is the decay rate of the alternating field. The dependence of the ARM of noninteracting particles on h is described by an acquisition function $L(h)$, with:

$$\lim_{h \rightarrow \pm \infty} L(h) = \pm 1, \lim_{h \rightarrow 0} L(h) = h, L(-h) = -L(h) \quad (6)$$

Egli and Lowrie [2002] found $L(x) = \tanh(x)$ for uniaxial SD particles.

[14] In the following, I introduce various parameters needed to calculate the ARM of interacting particles. The

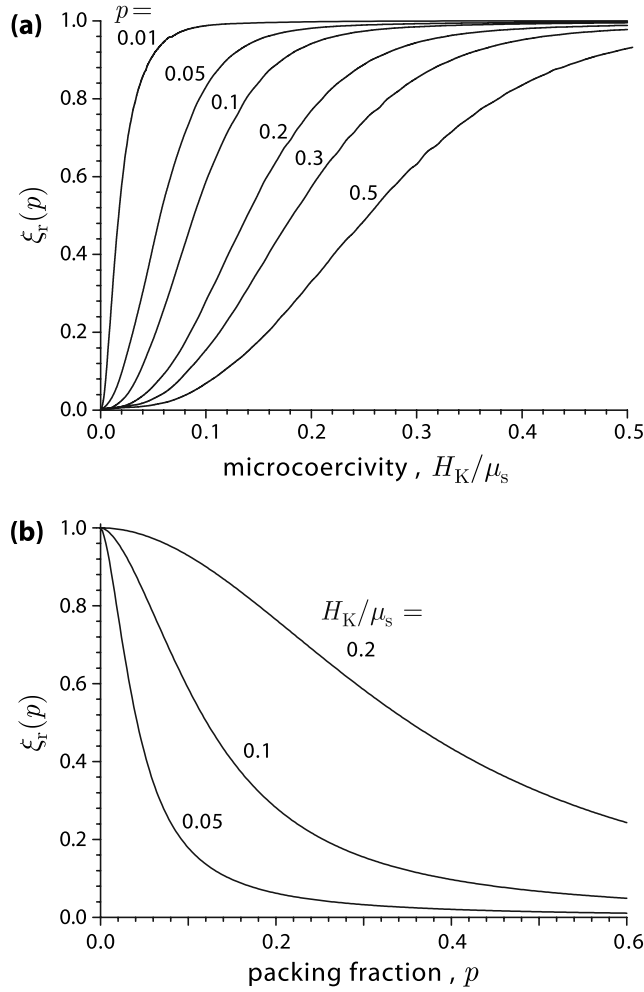


Figure 3. (a) Dependence of ξ_r (see text) on the microcoercivity H_K of the magnetic particles for selected packing fractions p . (b) Dependence of ξ_r on the packing fraction for selected values of the microcoercivity.

effective switching field distribution (SFD) of the particles is given by $M'_r(H_{sw})$, whereby H_{sw} does not necessarily coincide with the intrinsic switching field of isolated particles. The function $M'_r(H_{sw})$ represents the contribution of all particles with switching fields H_{sw} to the remanent magnetization of the sample. Similarly, $M'_a(h, H_{sw})$ is the contribution of all particles with switching fields H_{sw} to the ARM in the noninteracting case. According to this definition,

$$\begin{aligned} M_r(H_{sw}) &= \int_{H_{sw}}^{\infty} M'_r(H) dH \\ M_a(h, H_{sw}) &= \int_{H_{sw}}^{\infty} M'_a(h, H) dH \end{aligned} \quad (7)$$

are the saturation remanent magnetization and the anhysteretic magnetization of all grains with a switching field $> H_{sw}$. The ARM susceptibility of noninteracting particles with switching field H_{sw} is defined as $\chi'_a(H_{sw}) = M'_a(h, H_{sw})/h$ for $h \rightarrow 0$. The ARM susceptibility χ_a of all non interacting particles is given by the integration of χ'_a over all switching fields. By analogy, the quantities

M_{ai} , M'_{ai0} , χ'_{ai} , and χ_{ai} are defined for the interacting case (Table 1).

[15] The ARM acquired by noninteracting particles with switching field H_{sw} is given by:

$$M'_a(H_{sw}, h) = M'_r(H_{sw})L[\chi'_a(H_{sw}) h/M'_r(H_{sw})] \quad (8)$$

[16] To understand how (8) is modified in case of interactions, let us discuss the progress of the ARM process with time on an initially demagnetized sample. When the peak alternating field decays from its initial value \tilde{H}_0 to \tilde{H} , all grains with $\tilde{H} < H_{sw} \leq \tilde{H}_0$ have already acquired an ARM. Let $M_{ai}(\tilde{H}, h)$ be the ARM acquired by these grains. All other grains are still unblocked, and their moment is switched periodically by the alternating field. At this stage of the ARM acquisition, all grains with $H_{sw} = \tilde{H}$ are about to acquire a magnetization. These grains are subjected to an alternating IF produced by all unblocked particles, and a static IF produced by the blocked particles. The static IF can be calculated by assuming the sample to be composed only of the blocked particles. If the sample is homogeneous, the effective packing fraction of the blocked particles is given by $p(\tilde{H}) = pQ(\tilde{H})$, where $Q(\tilde{H}) = M_r(\tilde{H})/M_{rs}$, and PDF of the static IF is $W(H_i + fM_{ai}; pQ, \mu_s)$.

[17] The anhysteretic magnetization of all particles that block at \tilde{H} is acquired in a static field that is the sum of the bias field h and the static IF. Since the static IF is a statistical

Table 1. List of Symbols and Notations

Symbol	Explanation
H	total field acting on a particle
h	bias field during an ARM acquisition
\tilde{H}	alternating field during an ARM acquisition
H_d	demagnetizing field
H_i	local interaction field along a given direction
H_K	microcoercivity
H_z	random component of H_i
H_m	mean value of H_i
H_{sw}	switching field
$L(h)$	ARM acquisition function (noninteracting)
M	magnetization
$M_a(H_{sw})$	ARM magnetization curve (noninteracting)
$M_{ai}(H_{sw})$	ARM magnetization curve (interacting)
$M'_a(h, H_{sw})$	contribution of all particles with H_{sw} to the ARM (noninteracting)
$M'_{ai}(h, H_{sw})$	contribution of all particles with H_{sw} to the ARM (interacting)
$M_r(H_{sw})$	remanent magnetization curve
$M'_r(H_{sw})$	switching field distribution
p	packing fraction of the particles
Q	fraction of blocked particles during an ARM acquisition
$r'_a = \chi'_a/M'_r$	ARM ratio of all particles with given switching field (noninteracting)
$W(H, p, \mu_s)$	PDF for the local, random IF
χ_a	susceptibility of ARM (noninteracting)
χ_{ai}	susceptibility of ARM (interacting)
χ'_a	contribution of all particles with H_{sw} to χ_a (noninteracting)
χ'_{ai}	contribution of all particles with H_{sw} to χ_a (interacting)
μ_s	saturation magnetization of the particles

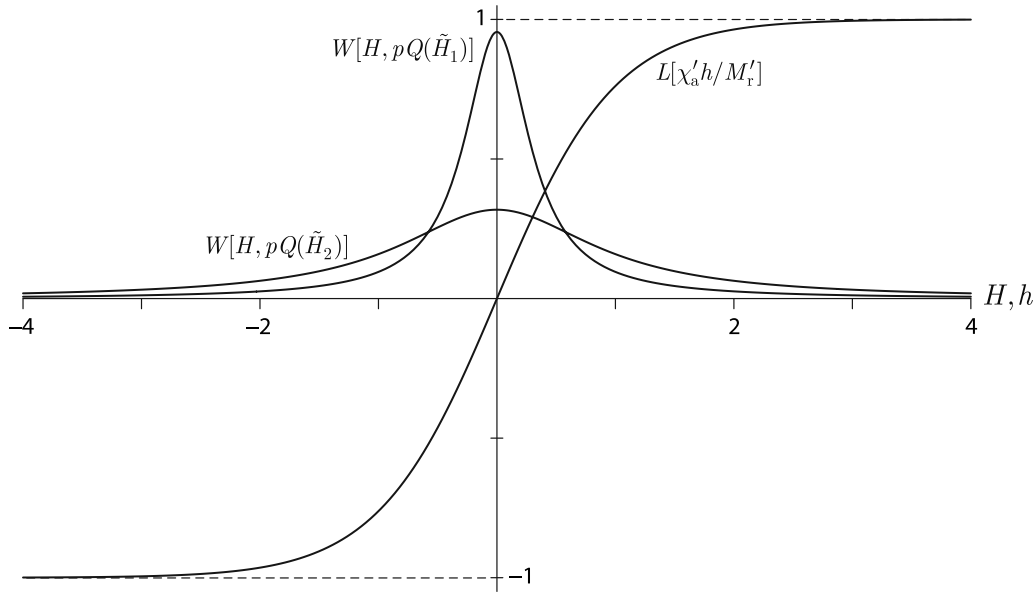


Figure 4. ARM acquisition function L and the distribution W of the random IF produced by the blocked particles when the amplitude of the alternating field is equal to \tilde{H}_1 and \tilde{H}_2 , respectively, whereby $\tilde{H}_2 < \tilde{H}_1$. The ARM acquired by all particles with switching fields equal to \tilde{H}_1 or \tilde{H}_2 is given by the convolution of L and W (see text).

variate, the magnetization acquired at \tilde{H} is obtained by integrating all possible configurations of the IF:

$$M'_{ai0}(\tilde{H}, h) = M'_r(\tilde{H}) \int_{-\infty}^{\infty} W[H + fM_{ai}; pQ, \mu_s] \cdot L[\chi'_a(\tilde{H})(h + H)/M'_r] dH \quad (9)$$

[18] The integral in (9) corresponds formally to the convolution of $W(x)$ and $L(x)$ (Figure 4). The noninteracting case is represented by $p \rightarrow 0$, whereby W becomes a Dirac δ function, and the integral is replaced by $L[\chi'_a(\tilde{H})h/M'_r]$. The same result is obtained for the interacting case when $H_{sw} \rightarrow \infty$, because the IF produced by the few blocked particles is small. The index “0” in (9) is used to remind that the left-hand side does not correspond to the final contribution M'_{ai} of all particles with a switching field $H_{sw} = \tilde{H}$. The difference between M'_{ai} and M'_{ai0} relies on the fact that (9) provides a statistical description of the switching state of the particles, assuming that the magnetic moments are parallel or antiparallel to the easy axis. As discussed in section 3, the IF deflects the magnetic moments from the easy axes. This effect is accounted by $M_{ai} = M'_{ai0} \xi_r$, where ξ_r was calculated in section 3. The magnetization M_{ai} is obtained by integrating $M'_{ai0} \xi_r$ over all switching fields, whereby the integral is complicated by the fact that M'_{ai0} is a function of H_{sw} and ξ_r is a function of H_K . In the case of Stoner-Wohlfarth particles, a good approximation is given by $H_K \approx 2H_{sw}$ [Stoner and Wohlfarth, 1948], and $M_{ai}(\tilde{H}) = M'_{ai0}(\tilde{H})\xi(\tilde{H})$ with

$$\xi(\tilde{H}) = \frac{1}{M'_{ai0}(\tilde{H})} \int_{\tilde{H}}^{\tilde{H}_0} \xi_r(2u)M'_{ai0}(u) du \quad (10)$$

Another assumption of (9) is that the SFD is unaffected by interactions. This assumption is reasonable for weakly

interacting samples, but is not necessarily true when the distance of the particles becomes comparable to their diameter [Muxworthy *et al.*, 2003]. I will show later that the result of (9) is nearly independent of the effective SFD of the sample.

[19] Let us assume $h \rightarrow 0$ in the following. Since $|fM_{ai}| < h$, (9) can be simplified using a first-order Taylor expansion of W and L with respect to fM_{ai} and h , respectively. The result of this linearization step is

$$M'_{ai0}(\tilde{H}, h \rightarrow 0) = (hf - M_{ai0}) \int_{-\infty}^{\infty} f \xi \chi'_a W(u) L'(\chi'_a u / M'_r) du \quad (11)$$

where L' is the derivative of L . Equation (11) is a linear differential equation on M_{ai} with general solution:

$$M_{ai0}(\tilde{H}, \tilde{H}_0, h) = hf + C \exp[-G(\tilde{H}, H_0)] \\ G(\tilde{H}, \tilde{H}_0) = \int_{\tilde{H}}^{\tilde{H}_0} \int_{-\infty}^{\infty} f \xi \chi'_a W(u; pQ, \mu_s) L'(\chi'_a u / M'_r) du dH \quad (12)$$

where C is an integration constant that satisfies the initial condition $M_{ai0}(\tilde{H}_0, h) = 0$. Since $G(\tilde{H}_0, H_0) = 0$, $C = -hf$. A complete ARM is acquired when $\tilde{H} = 0$ and the initial alternating field \tilde{H}_0 is sufficient to switch all particles. Using $\chi_{ai} = M_{ai}/h$, $\tilde{H} = 0$, and $\tilde{H}_0 \rightarrow \infty$, the following general solution is obtained from (12):

$$\chi_{ai} = \frac{\xi(0)}{f} \{1 - \exp[-G(0, \infty)]\} \quad (13)$$

[20] In the following, I will derive a simple expression for G , starting from the observation that $Q(\tilde{H})$ and \tilde{H} are equivalent variables. Thus all variables in (12) can be expressed as a function of Q (Figure 5). Using the scaling property $W(H_i; p, \mu_s) = W(H_i/\mu_s; p, 1)/\mu_s$ of the IF

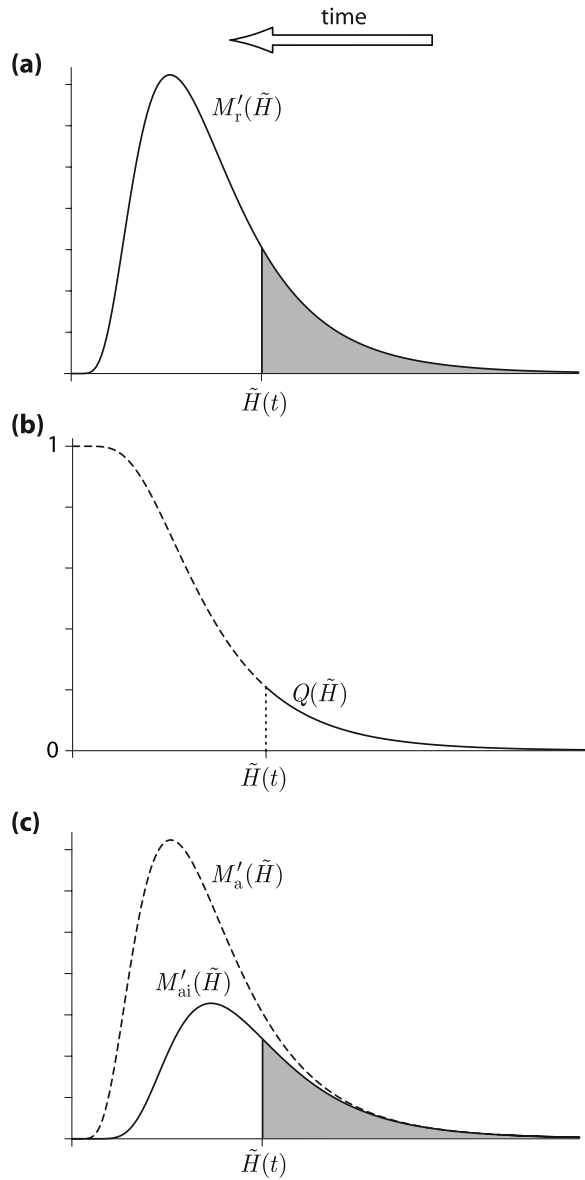


Figure 5. Schematic representation of the ARM acquisition process as \tilde{H} decreases from its initial value to zero. (a) Switching field distribution $M'_r(H_{sw})$. The dashed area represents the relative amount Q of blocked particles. (b) Relative amount Q of blocked particles. (c) Magnetic contribution of all particles with switching field $H_{sw} = \tilde{H}$ to the ARM for the noninteracting case (dashed line), and the interacting case (solid line). Since the IF produced by the blocked particles increases as \tilde{H} decreases, magnetic particles with a small switching field are less efficiently magnetized.

distribution [Egli, 2006], and defining the ARM ratio $r'_a = \chi'_a / M'_r$, equation (12) simplifies to

$$G(\tilde{H}, H_0) = fM_{rs} \int_{Q(\tilde{H}_0)}^{Q(\tilde{H})} r'_a \xi \int_{-\infty}^{\infty} W[u; pq, 1] L'(r'_a \mu_s u) du dq \quad (14)$$

where r'_a and $\xi = \xi[Q^{-1}(q)]$ are functions of q . Equation (14) does not have a general analytical solution. The first

simplification is obtained if $p \leq 0.01$. In this case, W is approximated by the Lorentz function given in (3), and, using $L(x) = \tanh x$, the integral on u in (14) can be solved. Using this solution,

$$G(\tilde{H}, H_0) = fM_{rs} \int_{Q(\tilde{H}_0)}^{Q(\tilde{H})} r'_a \xi \zeta_2 \left(\frac{1}{2} + \alpha p \mu_s r'_a / \pi \right) dq \quad (15)$$

where ζ_2 is the Hurwitz zeta function. Both x and r'_a in (15) are functions of the switching field $H_{sw} = Q^{-1}(q)$. A further simplification is obtained by considering the intrinsic properties of SD particles and their SFD. Egli [2004] used detailed measurements of ARM and isothermal remanent magnetization (IRM) of various sediments to calculate the SFD of natural magnetic components. The SFD calculated from measurements of ARM and IRM for each magnetic component have been found to be very similar, whereby the differences between the bulk AF demagnetization curves of ARM and IRM arose mainly from the different ARM ratios of the various components. Therefore r'_a depends only weakly on H_{sw} within each magnetic component. A physical explanation of this result relies on the fact that r_a is mainly a function of the particle volume [Egli and Lowrie, 2002] and depends only weakly on H_K . Furthermore, thermal fluctuation analysis of natural assemblages of SD grains shows that H_K is usually better constrained than the volume of the particles [Jackson et al., 2006]. Therefore I assume $r'_a(H_{sw}) \approx r_a$ to be a good approximation for natural assemblages of SD particles.

[21] The last difficulty in integrating (15) comes from the dependence of ξ on \tilde{H} , and is overcome by assuming $\xi = \xi_r(\bar{H}_K, p)$, where \bar{H}_K is the average microcoercivity of the particles. The effect of this approximations on the final result is negligible, as proved by comparison with a numerical integration of (15). If ξ and r'_a are constants, and $r_a M_{rs} = \chi_a$,

$$G(\tilde{H}, H_0) = f \xi_r \chi_a \int_{Q(\tilde{H}_0)}^{Q(\tilde{H})} \zeta_2 \left[\frac{1}{2} + \alpha \chi_a / (r\pi) \right] dq \quad (16)$$

[22] Using, $Q(\tilde{H}_0) = 0$ and $Q(\tilde{H}) = 1$ for a complete ARM acquisition,

$$G(0, \infty) = 2f r \xi_r \frac{\gamma + \ln 4 + \psi_0 \left[\frac{1}{2} + \alpha \chi_a / (r\pi) \right]}{\pi \alpha} \quad (17)$$

where ψ_0 is the digamma function, and $\gamma \approx 0.5772$ is the Euler constant. Inserting (17) into (12) gives the following final solution:

$$\chi_{ai} = \xi_r f^{-1} \left\{ 1 - \exp \left[-2f \xi_r r \frac{\gamma + \ln 4 + \psi_0 \left[\frac{1}{2} + \alpha \chi_a / (r\pi) \right]}{\pi \alpha} \right] \right\} \quad (18)$$

[23] Equation (18) is precisely valid for a homogeneous, isotropic sample of uniaxial particles with $p \leq 0.01$ and an ARM ratio that is independent of the switching field. However, the effect of the Lorentz approximation of the IF distribution introduced to obtain this result is negligible,

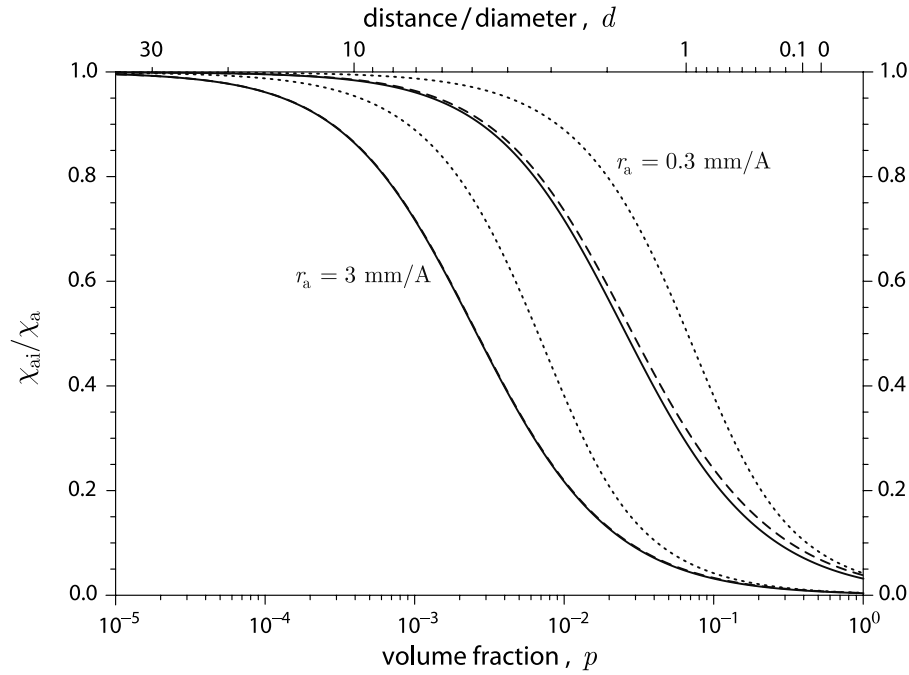


Figure 6. Comparison between the ARM calculated by numerical evaluation of equation (12) (dashed line) and the approximated solution (18) (solid line). The two curves overlap for values of the ARM ratio typical of SD magnetite ($r_a = 3$ mm/A). The mean-field solution calculated by Wohlfarth [1964] is shown for comparison (dotted line).

as shown by the comparison of (18) with a numerical evaluation of equation (12) (Figure 6). Therefore the validity range of (18) can be extended to all packing fractions. Interestingly, χ_{ai} does not depend on the coercivity distribution of the particles, because the entire ARM acquisition process can be expressed as a function of Q , which is independent from the coercivity distribution. An important consequence of this result is the possibility of ignoring the effect of interactions on the switching field distribution, thus eliminating one aspect of the nonlinearity of the problem.

[24] The noninteracting limit case is given by $p \rightarrow 0$, whereby $\chi_a \rightarrow 0$ as well, and (18) converges to $\chi_{ai} = \chi_a$, as expected. The opposite limit, given by $\chi_a \rightarrow \infty$, represents the case of strongly interacting particles. In this case, the solution of (18), $\chi_{ai} \approx \xi_r f^{-1}$, is completely controlled by the mean IF. Wohlfarth [1964] obtained a similar expression for the ARM of interacting particles:

$$\chi_{ai} = f^{-1} [1 - \exp(-f\chi_a)] \quad (19)$$

using a mean-field approximation of the IF. A comparison of the two solutions (18) and (19) shows that the mean-field approximation is correct only for $p > 0.1$, since the ARM of weakly interacting systems is controlled by the random component of the local IF. The weakly interacting case corresponds to the Presiach-Néel model of magnetostatic interactions [Néel, 1954], where the IF is a fixed statistical variate.

[25] Some examples of the dependence of χ_{ai} on the packing fraction, the ARM ratio, and the switching field of typical SD magnetite grains are shown in Figure 7. The ARM is strongly influenced by the packing fraction of the particles, whereby a measure of this effect is provided by

the packing fraction $p_{1/2}$ for which $\chi_{ai} = 0.5\chi_a$. For typical SD magnetite, $p_{1/2} = (3-8) \times 10^{-3}$ is obtained assuming $\mu_s = 480$ kA/m, $f = 1/3$, $r = 0.5$, and $r_a = 1-3$ mm/A. Noticeable interaction effects occur already at $p = (1-4) \times 10^{-4}$, which corresponds to a mean particle distance equal to ≈ 28 times their diameter. For comparison, micromagnetic simulations of cubic particle arrays did not show interaction effects on the hysteresis parameters for distances >3 times the particle size [Muxworthy *et al.*, 2003].

[26] The extreme sensitivity of ARM to interactions explains the low ARM ratios measured in synthetic samples of SD magnetite [Sugiura, 1979], because of the tendency of strongly magnetic particles to form clusters that are difficult to disperse. On the other hand, ARM ratios that are compatible with theoretical values for SD magnetite are commonly measured in sediments [Egli, 2004], showing that authigenic magnetites and maghemites are extremely well dispersed in most cases. This result allows a straightforward interpretation of ARM measurements as a granulometric indicator [e.g., King *et al.*, 1982] as well as its use for magnetic fabric investigations. However, examples of natural assemblages of strongly interacting particles have been found as well [e.g., Wehland *et al.*, 2005; A. P. Chen *et al.*, First-order reversal curve diagrams of natural and cultured biogenic magnetic particles, submitted to *Journal of Geophysical Research*, 2006].

5. Effect of Interactions on the Decay Rate Dependence and the Anisotropy of ARM

[27] In this section I will discuss how interactions affect the dependence of the ARM on various parameters, such as the decay rate η of the alternating field, the demagnetizing

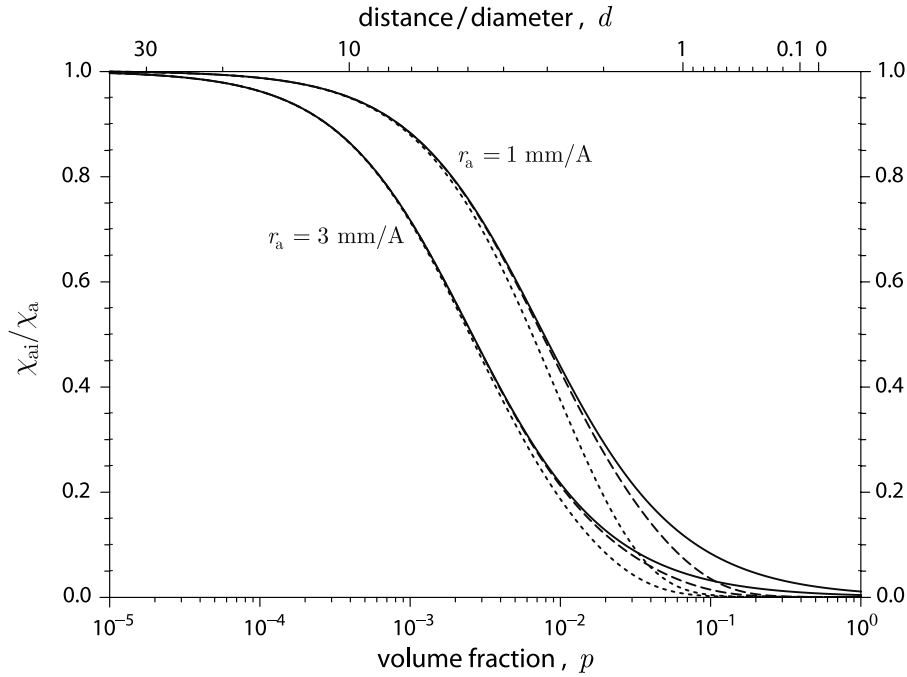


Figure 7. Dependence of the ARM susceptibility on the packing fraction p . The two sets of curves were calculated using $r_a = 1$ mm/A and $r_a = 3$ mm/A with $H_K/\mu_s = 0.05$ (dotted lines), $H_K/\mu_s = 0.1$ (dashed lines), and $H_K \rightarrow \infty$ (solid lines).

factor f , and the dispersion parameter α_0 of the IF distribution (3). The latter two parameters are influenced by the geometric arrangement of the particles, as discussed in section 2, and are responsible for distribution anisotropy effects on the ARM. In all cases I assume that the dependence of the ARM on one of these parameters is weak and can be expressed by a relative difference $\Delta\chi_{ai}/\chi_{ai} \ll 1$ of the ARM susceptibility measured at different orientations (magnetic anisotropy), or using different AF field decay rates.

[28] The first case is given by all situations where intrinsic differences $\Delta\chi_a/\chi_a$ of the ARM exist independently of interaction effects. Examples are given by the AF decay rate dependence [Egli and Lowrie, 2002; Yu and Dunlop, 2003], and anisotropy due to a preferred orientation of the easy axes [Potter, 2004]. The chain rule of derivatives

$$\frac{\Delta\chi_{ai}}{\chi_{ai}} = \frac{\partial\chi_{ai}}{\partial\chi_a} \frac{\chi_a}{\chi_{ai}} \frac{\Delta\chi_a}{\chi_a} = \kappa_\chi \frac{\Delta\chi_a}{\chi_a} \quad (20)$$

gives the relationship between the interacting and the noninteracting cases, whereby κ_χ is the “coupling constant” between the two. Using (18),

$$\kappa_\chi = \frac{2\xi_r(\xi_r - f\chi_{ai})\chi_a}{\pi^2\chi_{ai}} \psi_1 \left[\frac{1}{2} + \alpha\chi_a/(r\pi) \right] \quad (21)$$

where ψ_1 is the polygamma function. As discussed in section 4, the noninteracting limit is given by $\chi_a \rightarrow 0$, whereby $\kappa_\chi(\chi_a \rightarrow 0) = 1$, as expected. On the other hand, $\kappa_\chi \rightarrow 0$ in strongly interacting cases: intrinsic differences in χ_a are cancelled by the IF (Figure 8). If $\Delta\chi_a/\chi_a$ is related

to the anisotropy of the particles, the effect of interactions can be quantified using the degree of anisotropy

$$P = K_1/K_3 \quad (22)$$

and the shape parameter T of the anisotropy tensor [Jelinek, 1981],

$$T = 2 \frac{\ln(K_2/K_3)}{\ln(K_1/K_3)} - 1 \quad (23)$$

where K_1 , K_2 , and K_3 are the maximum, intermediate, and minimum values of the ARM. If the spatial distribution of the particles is isotropic, it can be easily shown that $P_i = \kappa_\chi P$ and $T_i \approx \kappa_\chi T$, where the index “i” is used to indicate the interacting case. As shown in Figure 8, $\kappa_\chi \approx 0.1$ for SD magnetite grains with a 1% volume concentration, and the degree of anisotropy, as well as the shape parameter, are reduced by a factor 10. The dependence of this effect on the microcoercivity of the particles is negligible for $p \approx 0.01$.

[29] The effect of distribution anisotropy is more complex. It requires a precise estimate of the IF distribution of anisotropic particle arrangements, which is beyond the scope of the present paper. A small degree of distribution anisotropy is produced by $\Delta f/f \ll 1$ and $\Delta\alpha/\alpha \ll 1$. The chain rule of derivatives can be used to evaluate the effect of distribution anisotropy on a set of particles with an isotropic distribution of easy axes. The effect of the demagnetizing factor is expressed by

$$\frac{\Delta\chi_{ai}}{\chi_{ai}} = \frac{\partial\chi_{ai}}{\partial f} \frac{f}{\chi_{ai}} \frac{\Delta f}{f} = -\kappa_f \frac{\Delta f}{f} \quad (24)$$

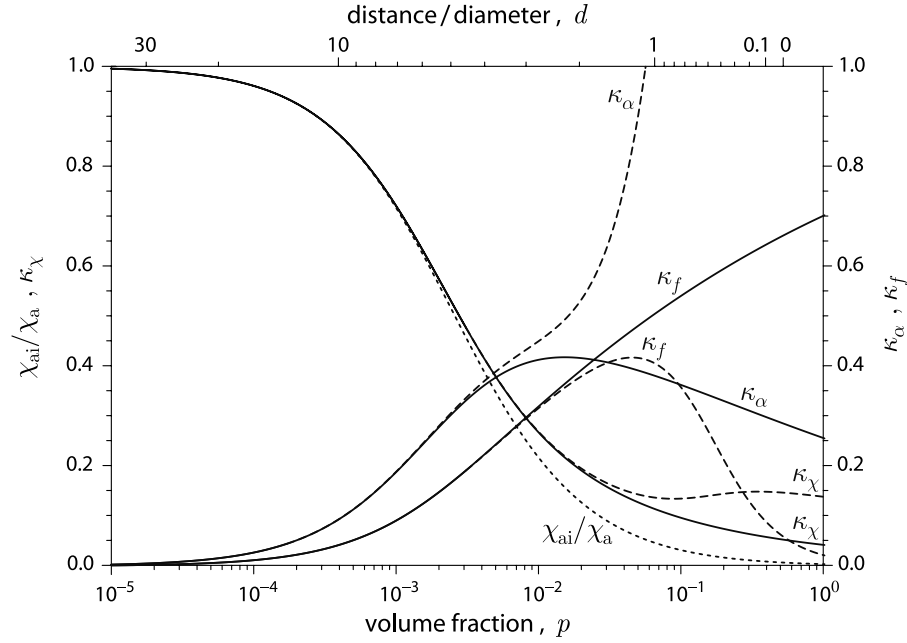


Figure 8. Factors κ_χ , κ_f , and κ_α affecting the AARM of interacting particles (see text for details). Solid lines refer to $H_K \rightarrow \infty$, and dashed lines refer to $H_K/\mu_s = 0.1$. The susceptibility of ARM is shown for comparison (dotted line). Other parameters used for the calculations are $\mu_s = 480$ kA/m, $f = 1/3$, $r = 0.5$, and $r_a = 3$ mm/A.

where κ_f is the “coupling constant” between the anisotropy of f and χ_{ai} . Using (18),

$$\kappa_f = -\frac{\partial \chi_{ai}}{\partial f} \frac{f}{\chi_{ai}} = 1 + \frac{\xi_r - f \chi_{ai}}{f \chi_{ai}} \ln(1 - f \chi_{ai}/\xi_r) \quad (25)$$

[30] The case of α is more complex, since $\xi_r(p)$ depends on α as well. The chain rule of derivatives gives

$$\frac{\Delta \chi_{ai}}{\chi_{ai}} = \frac{1}{\chi_{ai}} \left(\frac{\partial \chi_{ai}}{\partial \alpha} \frac{\Delta \alpha}{\alpha} + \frac{\partial \chi_{ai}}{\partial \xi_r} \frac{\partial \xi_r}{\partial p} \frac{\Delta p}{p} \right) = \kappa_\alpha \frac{\Delta \alpha}{\alpha} \quad (26)$$

[31] Since α and p are proportional, $\Delta \alpha/\alpha = \Delta p/p$, and

$$\kappa_\alpha = \frac{1}{\chi_{ai}} \left(\alpha \frac{\partial \chi_{ai}}{\partial \alpha} + p \frac{\partial \chi_{ai}}{\partial \xi_r} \frac{\partial \xi_r}{\partial p} \right) \frac{\Delta \alpha}{\alpha} \quad (27)$$

is the “coupling constant” between the anisotropy of α and χ_{ai} . Using (18), the explicit solution of (27) is

$$\kappa_\alpha = \frac{\xi_r - f \chi_{ai}}{f \chi_{ai}} \left\{ \frac{2f \xi_r \chi_a}{\pi^2} \psi_1 \left[\frac{1}{2} + \alpha \chi_a / (r\pi) \right] + \ln(1 - f \chi_{ai}/\xi_r) \right\} + p \frac{\xi_r'}{\xi_r} \left\{ 1 - \frac{\xi_r - f \chi_{ai}}{f \chi_{ai}} \ln(1 - f \chi_{ai}/\xi_r) \right\} \quad (28)$$

[32] In the limit case of no interactions, expressed by $\chi_a \rightarrow 0$, (25) and (28) give the intuitive result $\kappa_f \kappa_\alpha \rightarrow 0$. The evaluation of $\kappa_f(p)$ and $\kappa_\alpha(p)$ for typical SD magnetite grains ($\mu_s = 480$ kA/m, $f = 1/3$, $r = 0.5$, and $r_a = 3$ mm/A) shows that distribution anisotropy effects are negligible for $p < 10^{-4}$ (Figure 8). At intermediate concentrations, both κ_f and κ_α increase monotonically up to $p \approx 0.004$, whereby

the effect is independent of the microcoercivity of the particles. At higher packing fractions, both κ_f and κ_α become extremely sensitive to H_K . This result suggests that the effect of distribution anisotropy on the AARM of SD particles becomes difficult to predict when $p > 0.01$. On the other hand, a definitive evaluation of distribution anisotropy effects on the ARM is possible only when a precise model for the directional dependence of f and α allows combination of (25) and (28) to a single expression.

[33] *Muxworthy and Williams* [2004] used a micromagnetic model to calculate the effect of distribution anisotropy on the saturation isothermal remanent magnetization (SIRM). In their micromagnetic simulations of SD cubes, the anisotropy of SIRM (ASIRM) was strongly affected by distribution anisotropy at particle spacing smaller than the dimension of the cubes, which corresponds to $p > 0.125$. The limit for the onset of distribution anisotropy is obviously much smaller for the AARM, where measurable effects are expected for $p > 10^{-4}$ (Figure 8).

6. Conclusions

[34] An analytical model for the ARM of interacting SD particles has been developed. The model gives exact results in the limit case of weak interactions ($p < 0.06$). Realistic approximations were used to extend the validity range of the model to $p \rightarrow 1$. The ARM of SD particles is extremely sensitive to magnetostatic interactions, whereby the effects are noticeable at packing fractions as low as 10^{-4} , corresponding to a distance of the particles equal to ≈ 28 times their diameter. For comparison, hysteresis parameters are unaffected by interactions at $p < 0.01$.

[35] The effect of interactions on the AARM was investigated as well, whereby the measured anisotropy depend on

their spatial arrangement. An anisotropic spatial arrangement, expressed by the dependence of the average particle distance on the orientation of the sample, produces an unbalance between positive and negative interaction fields that modulates the directional dependence of ARM intensity. The AARM of SD particles is adversely affected by interactions when $p > 0.01$, whereby the dependence of the anisotropy parameter on p displays a complex behavior that depends strongly on p and on the microcoercivity of the particles.

[36] Additional work is needed to evaluate the effect of interactions on the anisotropy of remanence, whereby a combined use of AARM and ASIRM could provide better and more reliable information about the spatial arrangement of magnetic particles in natural samples.

[37] **Acknowledgments.** This work was supported by grant 0309291 from the Geophysics Program of the Earth Science Division of the National Science Foundation. I am grateful to Wyn Williams and David Potter for their constructive reviews. This is IRM publication 0608.

References

- Berkov, D. V. (1996), Local-field distribution in systems with dipolar interparticle interactions, *Phys. Rev. B*, *53*, 731–734.
- Della Torre, E., and F. Vajda (1997), Computation and measurement of the interaction field distribution in recording media, *J. Appl. Phys.*, *81*, 3815–3817.
- Egli, R. (2004), Characterization of individual rock magnetic components by analysis of remanence curves, 1. Unmixing natural sediments, *Stud. Geophys. Geod.*, *48*, 391–446.
- Egli, R. (2006), Theoretical aspects of dipolar interactions and their appearance in first-order reversal curves of thermally activated single-domain particles, *J. Geophys. Res.*, doi:10.1029/2006JB004567, in press.
- Egli, R., and W. Lowrie (2002), Anhysteretic remanent magnetization of fine magnetic particles, *J. Geophys. Res.*, *107*(B10), 2209, doi:10.1029/2001JB000671.
- Eldridge, D. F. (1961), Quantitative determination of the interaction fields in aggregates of single-domain particles, *J. Appl. Phys.*, *32*, 247S–249S.
- Hejda, P., and T. Zelinka (1990), Modeling of hysteresis processes in magnetic rock samples using the Preisach diagram, *Phys. Earth Planet. Inter.*, *63*, 32–40.
- Jackson, M. J., W. Gruber, J. Marvin, and S. K. Banerjee (1991), Detrital remanence inclination errors, and anhysteretic remanence anisotropy—Quantitative model and experimental results, *Geophys. J. Int.*, *104*, 95–103.
- Jackson, M., B. Carter-Stiglitz, R. Egli, and P. Solheid (2006), Characterizing the superparamagnetic grain distribution $f(V, H_c)$ by thermal fluctuation tomography, *J. Geophys. Res.*, *111*, B12S07, doi:10.1029/2006JB004514.
- Jaep, W. F. (1969), Anhysteretic magnetization of an assembly of single-domain particles, *J. Appl. Phys.*, *40*, 1297–1298.
- Jelinek, V. (1981), Characterization of the magnetic fabrics in rocks, *Tectonophysics*, *79*, T63–T67.
- Johnson, H. P., W. Lowrie, and D. Kent (1975), Stability of anhysteretic remanent magnetization in fine and coarse magnetite and maghemite particles, *Geophys. J.R. Astron. Soc.*, *41*, 1–10.
- Kneller, E. (1968), Magnetic-interaction effects in fine-particle assemblies and thin films, *J. Appl. Phys.*, *39*, 945–955.
- King, J. S., S. K. Banerjee, J. Marvin, and Ö. Özdemir (1982), A comparison of different models of determining the relative grain size of magnetite in natural materials: Some results from lake sediments, *Earth Planet. Sci. Lett.*, *59*, 404–419.
- Kodama, K. P. (1997), A successful rock magnetic technique for correcting paleomagnetic inclination shallowing: Case study of the Nacimiento Formation, New Mexico, *J. Geophys. Res.*, *102*, 5193–5205.
- Kodama, K. P., and W. W. Sun (1992), Magnetic anisotropy as a correction for compaction caused paleomagnetic inclination shallowing, *Geophys. J. Int.*, *111*, 465–469.
- Muxworthy, A. R., and W. Williams (2004), Distribution anisotropy: The influence of magnetic interactions on the anisotropy of magnetic remanence, in *Magnetic Fabric: Methods and Applications*, edited by F. Martín-Hernandez et al., *Geol. Soc. Spec. Publ.*, *238*, 37–47.
- Muxworthy, A., W. Williams, and D. Virdee (2003), Effect of magnetostatic interactions on the hysteresis parameters of single-domain and pseudo-single-domain grains, *J. Geophys. Res.*, *108*(B11), 2517, doi:10.1029/2003JB002588.
- Néel, L. (1949), Théorie du traînage magnétique des ferromagnétiques en grains fins avec applications aux terres cuites, *Ann. Geophys.*, *5*, 99–136.
- Néel, L. (1954), Remarques sur la théorie des propriétés magnétiques des substances dures, *Appl. Sci. Res., Sect. B*, *4*, 13–24.
- Néel, L. (1955), Some theoretical aspects of rock magnetism, *Adv. Phys.*, *4*, 191–243.
- Osborn, J. A. (1945), Demagnetizing factors of the general ellipsoid, *Phys. Rev.*, *67*, 351–357.
- Papuso, C., and A. Stancu (1993), Anhysteretic remanent susceptibility and the moving Preisach model, *IEEE Trans. Magn.*, *29*, 77–81.
- Potter, D. K. (2004), A comparison of anisotropy of magnetic remanence methods—A user's guide for application to paleomagnetism and magnetic fabric studies, in *Magnetic Fabric: Methods and Applications*, edited by F. Martín-Hernandez et al., *Geol. Soc. Spec. Publ.*, *238*, 21–35.
- Roberts, A. P., C. R. Pike, and K. L. Verosub (2000), First-order reversal curve diagrams: A new tool for characterizing the magnetic properties of natural samples, *J. Geophys. Res.*, *105*, 28,461–28,475.
- Rolph, T. C., and J. Shaw (1985), A new method of palaeofield magnitude correction for thermally altered samples and its application to Lower Carboniferous lavas, *Geophys. J.R. Astron. Soc.*, *80*, 773–781.
- Shaw, J. (1974), A new method of determining the magnitude of the paleomagnetic field application to 5 historic lavas and five archeological samples, *Geophys. J.R. Astron. Soc.*, *39*, 133–141.
- Shcherbakov, V. P., and V. Shcherbakova (1975), On the magnetostatic interaction in a system of single-domain grains, *Izv. Earth Phys.*, *9*, 101–104.
- Shcherbakov, V. P., B. E. Lamash, and N. K. Sycheva (1995), Monte Carlo modeling thermoremanence acquisition in single-domain grains, *Phys. Earth Planet. Inter.*, *87*, 197–211.
- Shcherbakov, V. P., N. K. Sycheva, and B. E. Lamash (1996), Monte Carlo modeling of TRM and CRM acquisition and comparison of their properties in an ensemble of interacting SD grains, *Geophys. Res. Lett.*, *23*, 2827–2830.
- Stephenson, A. (1994), Distribution anisotropy: Two simple models for magnetic lineation and foliation, *Phys. Earth Planet. Inter.*, *82*, 49–53.
- Stoner, E. C., and E. P. Wohlfarth (1948), A mechanism for hysteresis in heterogeneous alloys, *Philos. Trans. R. Soc. London, Ser. A*, *240*, 599–642.
- Sugiura, N. (1979), ARM, TRM, and magnetic interactions: Concentration dependence, *Earth Planet. Sci. Lett.*, *42*, 451–455.
- Walton, D. (1990), A theory of anhysteretic remanent magnetization of single-domain grains, *J. Magn. Mater.*, *87*, 369–374.
- Wehland, F., A. Stancu, P. Rochette, M. J. Dekkers, and E. Appel (2005), Experimental evaluation of magnetic interaction in pyrrhotite bearing samples, *Phys. Earth Planet. Inter.*, *153*, 181–190.
- Wohlfarth, E. P. (1964), A review of fine-particle interactions with special reference to magnetic recording, *J. Appl. Phys.*, *35*, 783–790.
- Xu, S., and D. J. Dunlop (1995), Toward a better understanding of the Lowrie-Fuller test, *J. Geophys. Res.*, *100*, 22,533–22,542.
- Yu, Y., and D. J. Dunlop (2003), Decay-rate dependence of anhysteretic remanence: Fundamental origin and paleomagnetic applications, *J. Geophys. Res.*, *108*(B12), 2550, doi:10.1029/2003JB002589.
- Yu, Y., D. J. Dunlop, and Ö. Özdemir (2002), Partial anhysteretic remanent magnetization in magnetite: 1. Additivity, *J. Geophys. Res.*, *107*(B10), 2244, doi:10.1029/2001JB001249.
- Yu, Y., D. J. Dunlop, and Ö. Özdemir (2002), Partial anhysteretic remanent magnetization in magnetite: 2. Reciprocity, *J. Geophys. Res.*, *107*(B10), 2245, doi:10.1029/2001JB001269.

R. Egli, Institute for Rock Magnetism, University of Minnesota, Minneapolis MN 55455, USA. (e.g.lix007@umn.edu)